Advancing Regional Flood Mapping in a Changing Climate: A HAND-Based Approach for New Jersey with Innovations in Catchment Analysis

D. Bazzett[1], Lucas Marxen[2], R. Wang[1*]

[1]Department of Civil and Environmental Engineering, Rutgers, The State University of New Jersey, New Brunswick, NJ 08904, USA

[2]SEBS/NJAES Office of Research Analytics, Rutgers, The State University of New Jersey, New Brunswick, NJ 08901, USA

Corresponding author: Ruo-Qian Wang (rq.wang@rutgers.edu)

Key Points:

- We created a calibration scheme for Manning's roughness using observed high-water marks and a regression to estimate roughness from geographic information.
- We developed a method to merge adjacent catchments to resolve the issues related to cross-boundary flow associated with the HAND model.
- Using measured precipitation data and modeled flow data, we developed a regression to estimate streamflow for future scenarios of increased precipitation.

Abstract

Regional flood mapping poses computational and spatial heterogeneity challenges, exacerbated by climate change-induced uncertainties. This study focuses on creating a state-wide flood mapping solution with enhanced accuracy and computational speed to support regional flooding hazard analysis and the assessment of climate change, using New Jersey as a case study. The Height Above Nearest Drainage (HAND) framework was employed for large-scale flood mapping. The model was validated against high water marks (HWMs) collected after Hurricane Irene. Based on the National Water Model (NWM), synthetic rating curves in HAND were calibrated by tuning Manning's roughness, aligning the predicted and observed flood depths. The roughness values were generalized across the state from the validated water basins to the ungauged ones, using a multivariate regression with the hydrologic and geographic information. To map the future climate-change-induced flooding, a correlation between NOAA historical precipitation totals and NWM flow data from 2010-2020 was established to link precipitation and runoff. This study also invented a novel method for correcting catchment discontinuities, inherent in the HAND model, based on a computer vision scheme, the Sobel filter. The modeling results show that average and worst-case storm events have the potential to increase 10-50% in the state, where mountain areas and major river banks would be exposed to this impact more significantly.

Plain Language Summary

In our study, we enhanced the Height Above Nearest Drainage (HAND) tool, which quickly generates flood maps by transforming stream flow data into detailed flood depth and reach information. The modeling tool is based on synthetic rating curves (SRC), which represent the relationship between flow and water depth based on the natural shape of river channels within a certain area.

A key challenge with HAND is that it relies on the Manning's Equation, which uses an assumed Manning's roughness coefficient. To get a more accurate estimate of the parameter, we fine-tune the Manning's roughness for many locations across New Jersey to better represent the appropriate roughness values for this equation. This model is proved reliable by comparing estimated depths to observed depths measured across the state at high-water marks (HWMs) and USGS depth gauges after Hurricane Irene. The tuned model is then applied to assess the future flooding impact of climate change and provides insights into the risk exposed at various locations in the state.

1 Introduction

Flooding is the most expensive and frequent natural disaster in the United States. In 2017, the total flood damages in the US were estimated at over US$300 billion (Smith, 2018), and the damage is expected to increase due to climate change in many parts of the world (Arnell, 2016; Swain, 2020). A common method to inform decision-makers about flood risk is through flood maps generated by intensive computational modeling, but the current flood maps are likely to be poorly suited for future use to reflect the impact of climate change. First, these models involve heavy computation, making them too slow for real-time flood forecasting to support emergency responses. Second, the heavy model needs high-resolution data and time-consuming iterations to

validate, and it is challenging to scale to a regional scale with enough details to support local responses.

For example, the popular hydraulic and flooding simulation tools, such as LISFLOOD and Hydrologic Engineering Center's River Analysis System (HEC-RAS), solve shallow water equations (SWE) to simulate flooding flows, requiring significant computational time and resources to resolve large-scale linear equation systems. They also require high-resolution data on local water infrastructure to represent local flooding processes. Considerable effort is also needed to update results if there are changes in landscape and hydraulic conditions. Moreover, constructing a flood model using these frameworks requires data that may not be available, such as cross-sections of channels and flood plains. It may require optimizing parameters such as friction coefficients. These limitations have hindered the development of real-time forecasting models (Ashfari et al., 2018; Zheng, 2018) and prevented supporting flood modeling in Earth System Models (Xu, 2022). So, there is a need to develop rapid and adjustable flood modeling tools with regional coverage and sufficient resolution.

Recent developments in terrain-based models, such as Height Above Nearest Drainage (HAND), provide an attractive solution for producing flood maps with similar results to these more complex models but requiring only a fraction of the computation resources and run time (Ashfari et al., 2018; Zheng, 2018). The HAND framework is a raster-based flood mapping system derived from a Digital Elevation Model (DEM) that can be used for flood mapping. This mapping is based on the method of Synthetic Rating Curves (SRCs) that estimate the relationship between flow and flood depth using Manning's equation (Liu et al., 2018; Maidment, 2016). Because the model is light in computation and the modeling unit is water catchments that can be adjusted independently, HAND could be easily updated to reflect the landscape and hydraulic condition changes and used to rapidly check a spectrum of climate scenarios. It also potentially supports real-time flood forecasting.

Despite five years of development, several issues remain in the HAND methodology and must be addressed before practical applications. First, assigning Manning's roughness values to each catchment/reach is challenging because flood data that can be used to validate flood models are usually rare and only available for a small fraction of the catchments. Two methods have been implemented in the past: 1) uniform roughness values were assigned across all catchments in a region (Ashfari et al., 2018; Johnson, 2019; Hocini, 2020), and 2) a range of roughness values were assigned based on landscape or the Strahler stream order of catchments (Li, 2016; Zheng, 2018) (the second reference did not discuss the method using stream orders, but the associated Github project did). However, Zheng (2018) and Johnson (2019) pointed out that HAND is sensitive to the accuracy of the roughness value, so careful selection of these values is needed to ensure the adequate performance of the model, and, more importantly, selecting the values requires validation using ground-truth data such as high-water marks, which are usually collected in the field immediately after flooding events, but this practice is not always performed.

Another issue with HAND is the flooding discontinuity across catchment boundaries, which tends to result in unrealistic flood depth distributions and underestimation of flood extent. For example, a catchment containing a small stream flowing into a much larger stream or river will not experience flooding if the larger stream floods – the catchment only floods from the single

stream segment it contains, and the catchment boundaries act as artificial barriers. This issue has been noted by others (Zheng, 2018; Johnson, 2019; Hocini, 2020) and will be discussed in detail in the present paper. To the best of the authors' knowledge, there have been no published attempts to resolve this issue, and this paper will be the first to address it using an innovative approach.

Despite the existing flood mapping tools that can convert precipitation to flow, there has been no systematic study to predict future flooding in various climate scenarios using such detailed flooding models, to the authors' knowledge. This gap may be partly due to the significant uncertainty surrounding climate change's impact on regional precipitation patterns. Several studies, including those conducted by Hatterman (2014), Arnell (2018), and Swain (2020), have modeled future flooding in different climate change scenarios in Germany, CONUS (Contiguous United States), and globally, respectively. Generally, flood risk is found to increase across most study areas, with possible decreases on a regional scale. However, the results have wide uncertainty due to variations in the scenarios utilized in each study. Additionally, generating flood maps on a regional scale is not common due to the large spatial scales and low resolutions of these studies. Since regional forecasting and a variety of climate change scenarios have become available recently, such as the Intergovernmental Panel on Climate Change (IPCC) Special Report Emissions Scenarios (SRES) or Representative Concentration Pathway (RCP) scenarios based on different CO2 emissions, it is now possible to quantify regional precipitation changes and translate them into information about future flooding.

A missing piece of information to support the effort to fill this knowledge gap is the large uncertainty in predicting future precipitation. Take New Jersey as an example, a report by Degaetano (2021a) analyzed historical rainfall data and concluded that since 2000, rainfall amounts have increased across much of the state for the 2-, 5-, 10-, 25-, 50-, and 100-year events. A separate study by Degaetano (2021b) used a series of climate simulations to determine how extreme rainfall may change in New Jersey and concluded that extreme precipitation may increase by 5-15% by the year 2100 under moderate emission scenarios or by as much as 15-30% under higher emission scenarios. Similarly, Daraio (2017) investigated streamflows and groundwater dynamics in two New Jersey watersheds amid varying climate scenarios. The study showed increased streamflow in both areas, aligning with the broader anticipated precipitation trends. Encouraged by these projections, our paper endeavors to employ the HAND approach for regional assessments, aspiring to present detailed flood risk data for towns and cities and the associated transportation system planning.

In this study, we created a calibrated HAND model for the state of New Jersey using high water marks (HWMs) to calibrate the Manning's roughness at discrete locations. In the following, Section 2 explains the methodology using geographic data at the locations with HWMs to create a multivariate regression to estimate roughness in regions where there was no HWM data. Section 3 shows model validation results using historical precipitation and flow data. Section 4 describes creating a forecasting model of precipitation and flow across New Jersey to create flow scenarios for different precipitation events. Using the flow data, we created flood maps for the different scenarios and developed a correction scheme to address the issue of missing transboundary flow in the HAND model.

2 Methods and Materials

2.1 Input Data

The basic HAND rasters of New Jersey used in the present study are a subset of the datasets hosted at the Oak Ridge National Laboratory (ORNL). These HAND rasters are based on the USGS (United States Geological Survey) 3DEP Digital Elevation Model with a 1/3 arcsecond (~10 m) spatial resolution and are split into catchments based on the National Hydrography Dataset (NHD) medium resolution data, with catchments generally ranging from 0.5-2 km² in area. The data for New Jersey is contained within the Hydrologic Unit Code (HUC) units of 020200, 020301, 020401, 020402, and 020403. The DEM data contains the elevation of the land surface but does not contain any bathymetry data underwater. Instead, it contains the water surface elevation when the DEM data was captured. Thus, zero values in the ORNL HAND data are set to be the water surface.

The stream flow rate data was obtained from the National Water Model (NWM), a continental-scale hydrologic model created by NOAA's Office of Water Prediction (OWP) using WRF-Hydro. The hindcast data includes flow estimates for every 1-hour timestep for each NHD catchment in the continental United States (Gochis, 2016). In addition, the NWM generates real-time forecast data to estimate future flows by assimilating USGS gauge data for accuracy, which can be coupled to provide real-time flood forecasts using the HAND model. Because the same NHD catchments are used in the NWM and ORNL HAND, the NWM flow data can be directly used to create flood maps using the ORNL HAND rasters. Data from version 1.2 of the NWM model was used for this study.

NOAA's Global Historical Climatology Network Daily (GHCN-D), a database of daily summary of climate data measured at stations around the world, is used in the present study to develop the correlation between precipitation and stream flow rates. For this study, we retrieved all stations located within New Jersey with precipitation data for the period of 2010-2020.

2.2 Model Calibration

Hurricane Irene was selected as a case study to validate the HAND model's accuracy. Hurricane Irene crossed New Jersey on August 27-30, 2011, flooding beyond the 100-year floodplain in many parts of the state (Watson, 2014). This event was chosen to validate the HAND model because it was an inland flood that is suitable to compare with the HAND model, and the data set for this event has a relatively good quality for the state. Specifically, two sets of high-water marks (HWMs) are used in this study: 1) following Hurricane Irene, USGS staff collected HWMs at various locations across New Jersey (Watson, 2014), which consist of silt stains, debris lines, or other indication of the maximum water depth with coordinates, 2) similar HWMs were collected by agents of Somerset County, New Jersey (provided via direct correspondence with the local USGS office). These HWMs were generally collected on larger river/stream sections in populated areas, typically at the four corners of vehicle bridges traversing rivers. The HWM dataset had the coordinates and elevation of each of the HWM features identified. There were 958 HWM points available from the USGS and 84 HWMs of similar quality collected within Somerset County by state agents.

In addition to the HWM data, 138 USGS stream gauges across New Jersey were available to record stream depth during the hurricane. The data during Hurricane Irene (Aug 27-31, 2011) was retrieved for each gauge, and the maximum depth during this period was determined for each gauge. This maximum depth was considered the local high-water level, similar to an HWM.

The HWMs were contained within 190 catchments, typically containing multiple points. The USGS gauges were present within 130 catchments. Among them, 33 catchments had both HWM and USGS data points. In total, 298 out of over 10,000 catchments (<3%) within New Jersey have at least one data point for validation. For comparison, the HWM point data was converted into HAND depths by comparing the HWM elevation to the local DEM elevation. The obtained difference was then compared with the local HAND flood depth.

For Aug 27-31, 2011, the hourly flow estimates for every catchment in New Jersey were retrieved from the NWM reanalysis data (v1.2). The maximum flow during this period was extracted for each catchment in New Jersey, and we assume that for a given catchment, the highest flow rate will result in the water level that creates the HWM.

A preliminary validation showed that using the default, uniform roughness of 0.05 from the ORNL dataset, the HAND model produced a flooding result poorly compared with the validation data. We believed that this disagreement between predictions and observations was primarily due to the roughness values of the synthetic rating curves provided. As mentioned earlier, an alternative approach to determine Manning's roughness in HAND involves estimating the values using the Strahler stream order, with low-order streams having greater roughness than higher-order streams (Zheng, 2018* [see note]; Li, 2016). But still, we found the method unsatisfactory, and a more accurate method is needed.

To achieve an improved strategy for assigning the roughness values, we developed a method to calibrate each catchment's roughness individually. Specifically, a Python-based optimization routine was created to calibrate the roughness of each catchment by minimizing the Root Mean Square Error (RMSE) between predicted and observed depths. As each catchment typically contained multiple HWMs with a range of HAND depths, the optimized depth typically would correspond to the average of the individual HAND depths. The lower and upper limits of the roughness were bounded to 0.005 and 0.200, which are more generous than typical roughness values in natural channels but intended to compensate for exceptional processes that the model is not designed to physically model and errors within either the NWM or HAND data. Optimized roughness values were determined for the 195 catchments with HWM data and the 136 catchments with USGS gauge data. After calibration, the predicted depths were in close agreement with the observed depths shown in Section 3.

Since only less than 3% of catchments have HWMs to calibrate, a quantitative method is demanded to determine the roughness in the remaining ~10,000 catchments in New Jersey, where no HWM or gauge data is available. We developed a multivariate linear regression to estimate the roughness in these catchments from the local landscape and hydrologic data. First, the Strahler stream order available in the NHD Value Added Attribute (VAA) dataset (USGS, 2019) was used as a categorical variable. Second, from the HAND SRC tables, the channel slope of each catchment was retrieved as the second variable for regression. Third, each catchment's

241 average latitude, longitude, and elevation were used to represent the geographic location in the
242 regression. The National Land Cover Database (NLCD) contains the majority land cover of each
243 catchment, and typical Soil Conservation Service (SCS) runoff curve numbers for each NLCD
244 land cover were trialed to build the multivariate linear regression. However, we found they could
245 not contribute to improving the validation significantly, so they were not included in the final
246 regression. We used linear regression to extrapolate the roughness values, so no overfitting
247 problem is expected.
248

249 2.3 Climate Scenario Data

250 A primary goal of this study is to estimate future flooding according to different climate
251 scenarios. Since HAND is a tool to translate stream flow data into flooding, stream flows under
252 future climate scenarios are needed to analyze the climate change impact on flooding estimates.
253 Although stream flow predictions under future climate scenarios are available, such as the
254 Climate Hydrology Assessment Tool (CHAT) (https://climate.sec.usace.army.mil/chat/), the tool's
255 results are still very preliminary with limited coverage, and the developers advised against
256 directly using their dataset for flooding purposes after consulting the team.
257
258 Given that the stream flow in most catchments in New Jersey strongly depends on the
259 precipitation (Anderson, 2023), we developed a strategy to make climate forecasts using a range
260 of precipitation levels with different climate scenarios. This approach enables us to make a first-
261 order estimate of flooding that can address the uncertainties inherent in climate forecasting.
262 Specifically, we built a linear correlation model to relate precipitation to streamflow within New
263 Jersey using the data from 2010-2020. Then, we applied the calibrated HAND model to translate
264 the various stream flow into flooding estimates. The daily precipitation data of the GHCNd
265 within New Jersey from 2010-2020 was retrieved from 740 gauges across the state to perform
266 the statistical analysis because the number of precipitation monitoring sites increased around
267 2010 and has been kept stable since then. Due to the sparsity of the precipitation gauges, the
268 precipitation data was estimated for each catchment using 2-D linear interpolation.
269
270 To build the correlation between precipitation and stream flow, we retrieved the hourly hindcast
271 data of NWM stream flow for the catchments within New Jersey for the same period as the
272 GHCNd data. A peak detection scheme was utilized to identify individual "rainfall" events (an
273 example is shown in Figure 1), allowing us to pair the maximum precipitation and maximum
274 flow rate for each event for the subsequent analysis. Using this data, we created linear models for
275 each catchment between the maximum precipitation and maximum flow rate and between the
276 average precipitation and average flow rate (example in Figure 2).

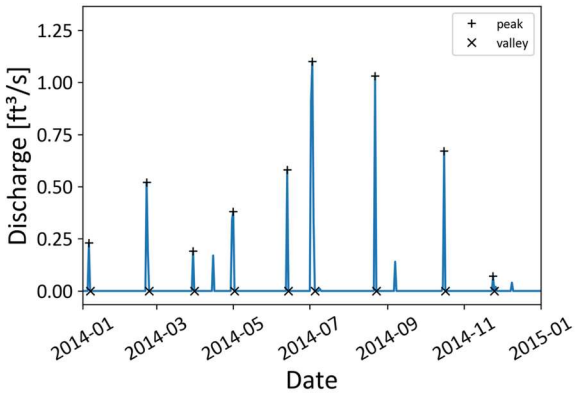

Figure 1: Sample of precipitation event detection and separation ("+" is event peak discharge; "x" is event date separator)

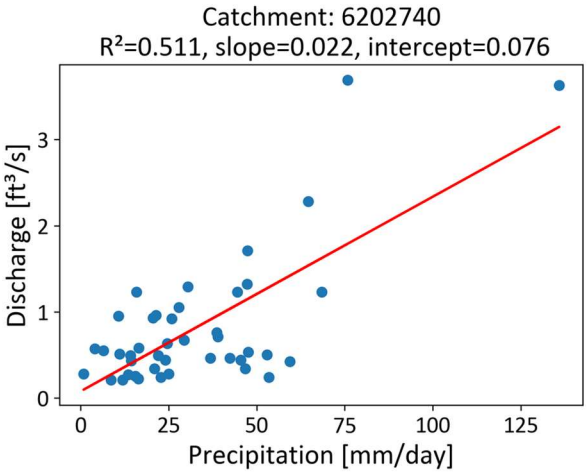

Figure 2: An example of the regression between precipitation and discharge.

Once the linear regression models were built for each catchment, extra precipitation of 10%, 20%, 30%, 40%, and 50% increases were used to extrapolate the model to these average and maximum scenarios. A total of 12 flood maps were created for the state of New Jersey using the flow data and the calibrated HAND model.

2.4 Addressing cross-boundary flooding issues

After the flood maps had been generated, discontinuity errors were found in the flood maps. This is an inherent issue in the HAND model that flooding in catchments cannot overflow into adjacent catchments – catchment boundaries act as solid barriers, and flood maps show sudden changes in flood depth that do not correspond to physical processes. An example is shown in Figure 3. In this example, Catchment 1 has a major river and a large water depth, while Catchment 2 only has a tributary which has a much smaller stream flow and thus a much lower water depth. As a result, a boundary forms between these two catchments. In comparison, if flooding water could freely flow between these two catchments, Catchment 2 would have a continuous water depth extended from Catchment 1. Two methods were developed to address these discontinuities: Method 1: For discontinuities along a continuous length of the stream, the depth was averaged across two upstream and two downstream catchments. Method 2: For discontinuities where a smaller stream joins a larger stream, a new method for identifying sharp edges and correcting them was created using the Sobel filter, an edge-detection technique common in computer vision (Sobel, 2014).

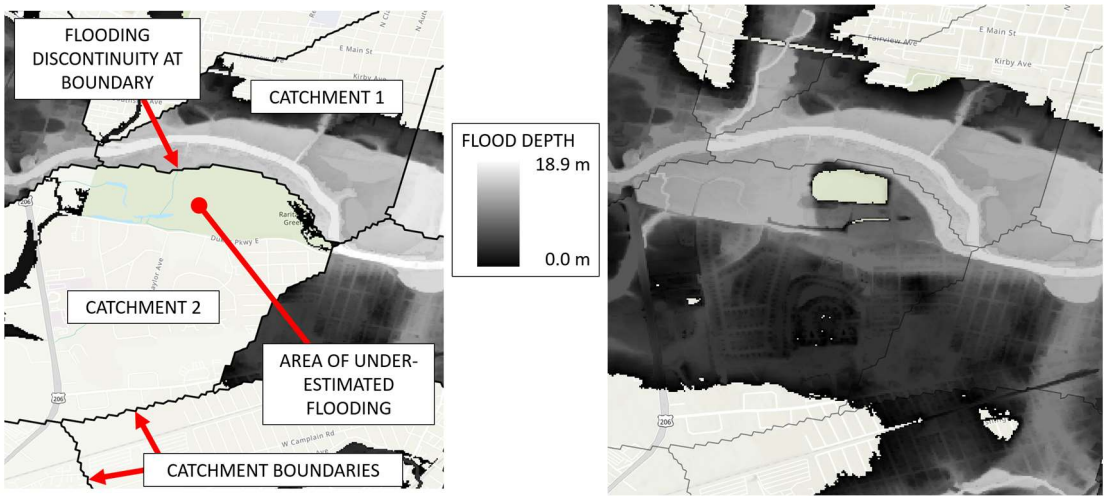

Figure 3: Discontinuities of flooding at the borders of catchments before (a) and after (b) merging

The Sobel filter was applied to each flood map, creating an image with the same dimension as the original flood map with values representing the water elevation gradient across pixels, or how quickly flood depth changes. The Sobel filter returns large values when the flood depth changes suddenly, which usually represents the artificial edges associated with the boundary flooding problem.

From experimenting, a Sobel value of 2.0 or greater was used as the threshold for which we should attempt to correct the flooding discontinuity. When this value was encountered, our Python script determined if the edge was located at the intersection of two different catchments. With the catchment ID numbers, the stream order for each catchment was retrieved from the NHD dataset. The smaller order catchment was then merged into the larger order catchment. The merging process consisted of recalculating HAND in the lower-order catchment relative to the higher one. This recalculation was done by approximating elevation differences, rather than flow paths for each pixel for computational convenience. Once the HAND was recalculated, inundation was mapped onto the new combined catchment using the inundation depth of the larger order catchment.

Both correction methods improved the flood maps from a qualitative perspective. Note that quantitative analysis of these methods was not performed because there was no ground truth data of flood coverage in New Jersey to compare against Hurricane Irene in all the corrected catchments.

3 Results

3.1 Model Validation

The calibration results for all catchments are shown in Figure 4, exhibiting the predicted and observed depths after calibration of Manning's roughness. We note that the minimum slope value must be increased from 0.00001 to 0.00003 to achieve a better fit for the higher-order stream. The RMSE of the calibrated data was 0.71m, an improvement upon an RMSE of 2.6m using the uniform roughness value.

The calibration results are summarized against the stream order in **Error! Reference source not found.**, showing the mean and median calibrated roughness values and errors for each stream order for the HWM and USGS gauge data. Figure 4 shows the boxplots of the roughness values for each stream order. Note that the lower stream order generally indicates that the stream has less flow and a smaller contributing area (watershed). Figure 5 shows that the roughness generally decreases with higher stream orders, which is consistent with the observation that the smaller channels are rougher and have more resistance to the flow. The average and median RMSE values also generally decrease as the stream order increases, but stream order 6 is an exception with higher RMSE values. The calibrated roughness is generally within the reasonable range. The only exception is the median and average calibrated roughness values for stream order 1, which are equal to or close to the upper bound of 0.2. This result seems unrealistic due to the relatively large uncertainty in the hydrologic and DEM data for the small tributaries.

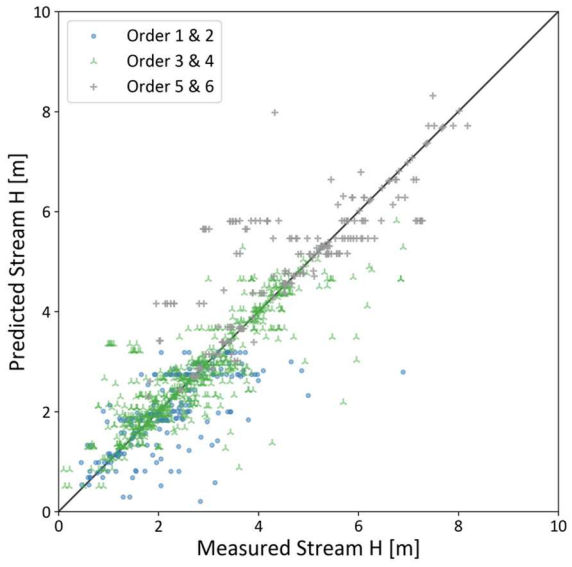

Figure 4: Calibration of the HAND model shows a good comparison between the predicted and measured stream heights (R^2=0.79, RMSE=0.71m)

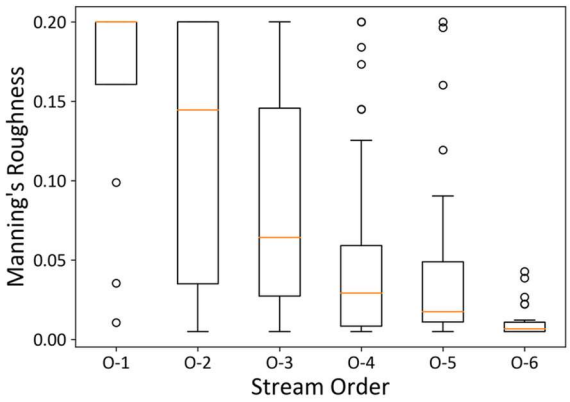

Figure 5: Distribution of the calibrated Manning's roughness within the bounds of 0.005 to 0.200 for different stream orders.

Table 1: Optimization results after cleaning

Manning's Roughness Statistics					
Order	Avg. Rough	Avg. RMSE (m)	Med. Rough	Med. RMSE (m)	Number of Catchments
1	0.159	0.83	0.200	0.87	13
2	0.117	0.52	0.145	0.32	58
3	0.088	0.42	0.064	0.21	91
4	0.050	0.35	0.029	0.18	71
5	0.047	0.18	0.018	0.06	25
6	0.011	0.68	0.007	0.30	28
All	0.077	0.55	0.043	0.21	286

3.2 Roughness estimates

As mentioned earlier, less than 3% of catchments have HWMs or gauge data to validate, so a regression model was developed to estimate the roughness of the catchments that have no HWM or gauge available. Table 2 lists all the attributes used in the multivariate regression with their weights. The regression used these attributes to estimate the calibrated roughness values obtained in the previous section. The results show that the most important factor in determining the roughness is the stream surface slope – greater slope results in higher roughness. This result indicates that steeper catchments often have stronger resistance to flows. The second important factor is geolocation, i.e., the longitude and latitude in Table 2. The positive weight in the longitude and the negative weight in the latitude suggest that the roughness decreases toward the northwest of NJ. This trend can be partially explained by the fact that NJ's north and west sides include major rivers, such as the Delaware River, Hudson River, and Passaic River, where Manning's coefficients are relatively small in these wide and deep channels. The elevation plays a non-trivial role in the regression, which means the rivers in mountainous areas tend to have stronger resistance to flows as expected. Also, a surprising result is that stream orders play a relatively weak role in determining the roughness, with lower orders tending to increase the roughness. This trend is consistent with the pattern for stream orders. After estimating roughness values for all catchments in New Jersey using this regression, estimated values outside the bounds of 0.005 and 0.200 were set equal to the bounding values.

3.3 Flooding Prediction for Future Climate Scenarios

The precipitation-streamflow regressions created across the state show strong spatial variability in the slope of these linear models (Figure 7): greater slopes indicate higher sensitivity of river discharge to precipitation. Flatter sections of southern New Jersey tend to have less sensitivity of discharge to precipitation than the northern areas with greater elevation variability. Large rivers showed a stronger sensitivity to precipitation, which results from the fact that these larger streams have a larger contributing area, so a rainfall event likely results in greater changes in flow. Since the catchments with higher sensitivity are likely to suffer from greater floods, the sensitivity distribution, to an extent, indicates the catchments' vulnerability over the state.

Table 2: Regression Weights

Normalized Weights	Parameter
0.911	Stream Surface Slope
0.408	Average Catchment Longitude (X)
-0.748	Average Catchment Latitude (Y)
0.327	Average Catchment Elevation (Z)
0.173	Stream Order 1
0.111	Stream Order 2
0.031	Stream Order 3
-0.093	Stream Order 4
-0.033	Stream Order 5
-0.188	Stream Order 6

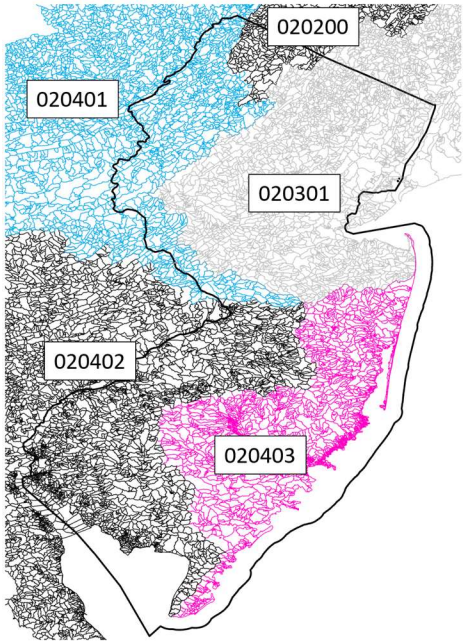

Figure 6: The five HUC6 catchments of New Jersey

Figure 8 shows the R^2 fit of the linear model across the state. The linear models perform well in the state's northern region but perform poorly in much of the southern region. This might be attributed to the flat topography that precipitation doesn't result in immediate high flow but surface water ponding or groundwater recharge.

Table 3 shows the inundated area in each NJ region (see Figure 6 for the geolocation of the HUC numbered areas). For each map, the inundated areas are calculated by multiplying the number of inundated pixels by 7.9 m x 7.9 m, the latitude-adjusted area of a 1/3 arcsecond pixel. Table 4 shows the inundation percentage increase for each HUC6 catchment. Across the state, each additional 10% of precipitation in the average storm scenarios results in a 1.3%-2.5% increase in inundated areas. In all catchments except 020200, the marginal increase in the inundated area generally decreases for the higher precipitation scenarios. This is somewhat intuitive as the terrain is generally a V-shaped channel: when the channel fills, more water is needed to provide the same increase in flooding extent. For the average storm plus 50% additional precipitation, the increase in the inundated area ranges from 9.5% to 10.9%. For the worst-case storms, the trends are largely the same, but with larger marginal increases in the inundated area ranging from 1.6%-3.3% for each 10% increase in precipitation, resulting in total increases of 9.1%-14.6% for the scenario with an additional 50% precipitation. This trend is shown in Figure 9 and Figure 10.

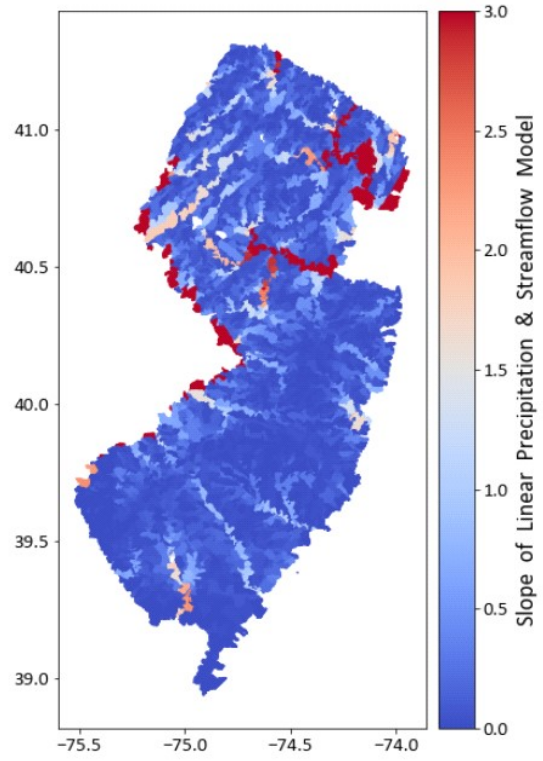

Figure 7: Slope of the linear regression models for each catchment.

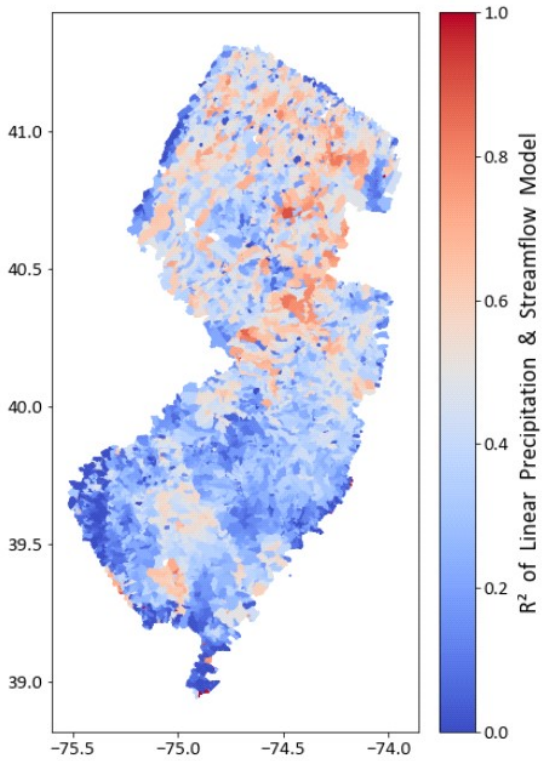

Figure 8: R^2 of the linear regression models for each catchment.

399

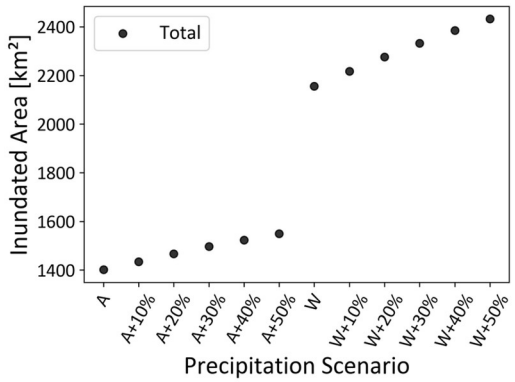

Figure 9: Total inundated area in NJ for each of the average (A) and worst-case (W) precipitation scenarios

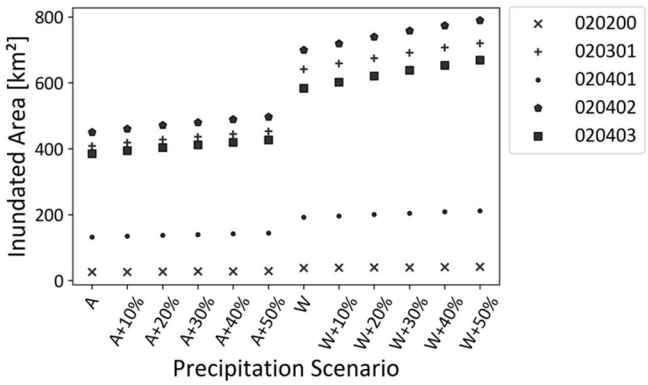

Figure 10: Inundated area by HUC6 in NJ for each of the average (A) and worst-case (W) precipitation scenarios

400

401 Table 3: Inundation area (km²) for the different HUC6 catchments under the different scenarios.

	020200	020301	020401	020402	020403	Total
Avg Storm	26.1	408.7	131.7	449.8	385.0	1401.3
Avg Storm + 10%	26.5	418.8	134.6	460.3	394.6	1434.8
Avg Storm + 20%	26.9	427.7	137.5	471.1	403.5	1466.7
Avg Storm + 30%	28.0	436.7	139.7	480.1	411.9	1496.4
Avg Storm + 40%	28.3	444.8	142.1	489.1	419.6	1523.8
Avg Storm + 50%	28.8	453.3	144.2	496.8	426.9	1550.0
Worst Storm	38.4	641.4	192.0	699.8	583.6	2155.1
Worst Storm + 10%	39.1	658.8	196.4	719.4	602.7	2216.4
Worst Storm + 20%	39.9	675.0	200.7	739.3	620.8	2275.8
Worst Storm + 30%	40.5	690.9	204.8	758.3	638.4	2332.9
Worst Storm + 40%	41.1	707.2	208.6	774.2	653.7	2384.8
Worst Storm + 50%	41.9	720.1	212.3	789.9	668.7	2432.9

402

403 Table 4: Cumulative percent increase in inundated area for the HUC6 catchments

	020200	020301	020401	020402	020403	Total
Avg Storm	0.0%	0.0%	0.0%	0.0%	0.0%	0.0%
Avg Storm + 10%	1.7%	2.5%	2.2%	2.3%	2.5%	2.4%
Avg Storm + 20%	3.3%	4.6%	4.4%	4.7%	4.8%	4.7%
Avg Storm + 30%	7.2%	6.8%	6.1%	6.7%	7.0%	6.8%
Avg Storm + 40%	8.6%	8.8%	7.9%	8.7%	9.0%	8.7%
Avg Storm + 50%	10.4%	10.9%	9.5%	10.5%	10.9%	10.6%
Worst Storm	0.0%	0.0%	0.0%	0.0%	0.0%	0.0%
Worst Storm + 10%	1.7%	2.7%	2.3%	2.8%	3.3%	2.8%
Worst Storm + 20%	3.8%	5.3%	4.6%	5.6%	6.4%	5.6%
Worst Storm + 30%	5.4%	7.7%	6.7%	8.4%	9.4%	8.2%
Worst Storm + 40%	7.1%	10.3%	8.7%	10.6%	12.0%	10.7%
Worst Storm + 50%	9.1%	12.3%	10.6%	12.9%	14.6%	12.9%

404

405 ## 3.4 Flood mapping and discontinuity correction

406

407 Using the tools included in the ORNL toolbox, the process of creating a flood map from flow
408 data can be accomplished quickly, i.e. in the order of seconds. The merging script can take up to
409 30 minutes to resolve issues in a single map, but improvements to the script could reduce this
410 time. An example of an area improved by merging is shown in Figure 3.
411
412 A qualitative comparison with the available FEMA flood maps overlain on the merged HAND
413 maps (Figure 11) showed that the FEMA flood maps reasonably agree with the shape and extent
414 of worst-case flood maps. The HAND flood maps for the worst-case scenarios with excessive
415 precipitation exceed the FEMA 100-year flood plain (Zone AE) in many places, indicating that
416 extreme scenarios of future climate change could overtake the past extreme prediction.
417
418 Figure 12 shows the change in the number of edges in a catchment after merging. This is
419 quantified for each pixel by determining the maximum difference in depth for the surrounding 8
420 pixels, both before and after merging. The statistic of the sharp edges is shown as a percentage of
421 the pre-merge counts. Generally, the merging reduces the sharpest edges (depth changes greater
422 than 5.0 m) and increases the number of pixels with less discontinuity. HUC 020401 is an
423 exception due to new sharp edges created on the boundary with another catchment.
424
425 The results of merging using different Sobel thresholds are summarized in Figure 13. A Sobel
426 threshold of 3.0 was used for the finished maps. This value was determined because it largely

removes the significant discontinuity in the map but without heavy computation. As shown in the figure, the threshold of 4.0 provides the smallest improvement to the base maps, with <0.27% additional inundation in the average scenarios and up to 4% increase in the worst case. For a threshold of 3.0, the increase is up to 0.64% in the average cases, and up to 5.8% for the worst cases. For a threshold of 2.0, the increase is up to 2.3% in the average cases and 8.0% for the worst cases. The computation time to process all maps for Sobel thresholds of 2.0, 3.0, and 4.0 was 1225, 725, and 315 minutes, respectively.

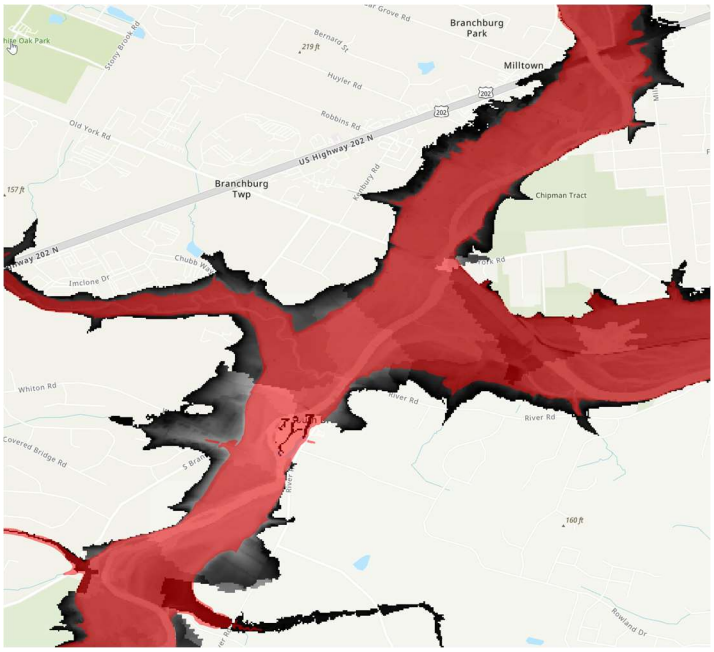

Figure 11: Merged flood map for worst case + 50% precipitation (darker) with FEMA Zone AE overlaid (lighter)

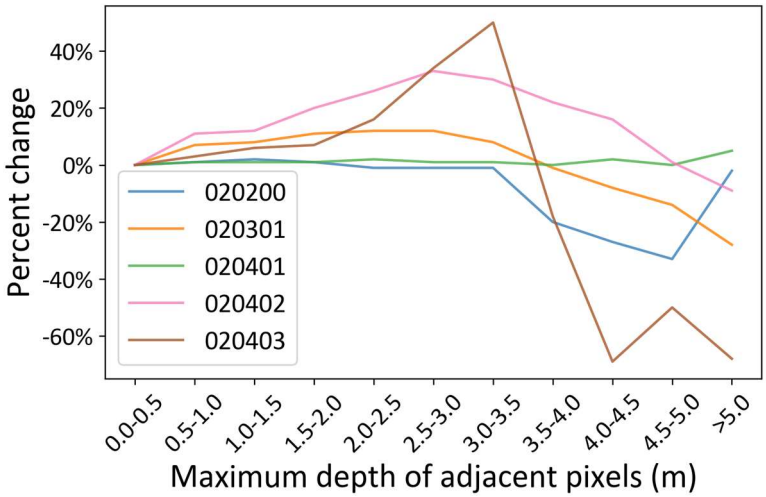

Figure 12: The fractional change in the number of pixels with a maximum adjacent depth after merging with sobel threshold = 3.0. The largest edges are reduced in four of five catchments after merging.

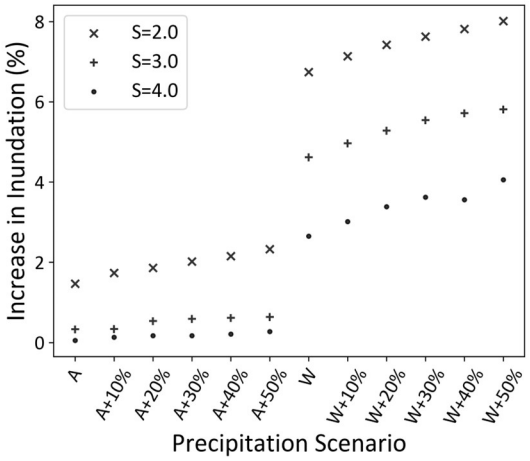

Figure 13: Increases in inundated areas after merging using different Sobel filter thresholds (S)

4 Discussion

The Manning's roughness is limited to 0.200, which represents the physical limits, but we observed that outliers exist following the model validation process. The non-physical values for the roughness might be attributed to inaccurate estimation of flow data or the rating curve, the channel geometry, and slope. Specifically, under-estimation of flow or over-estimation of geometry or slope could result in high roughness values in the calibration process. In addition, although the average roughness values from our calibration are consistent with other research that uses an inverse relationship between roughness and stream order, the variability of roughness values indicates that a single roughness value may lead to errors when generalizing by stream orders. This trend suggests some errors or non-physical data exist in the data pipeline. Extra errors could also be introduced by establishing the SRCs, which may not accurately capture the geometry of the channel due to the measurement restriction that the channels were not "empty" but instead contained some depth of water when the DEM data was captured. It is also noteworthy to mention that the slope data in the ORNL HAND data is taken from the NHD dataset, but this may not reflect the energy slope during a flood event.

We also note that the roughness values calibrated from the USGS gauge data were generally higher than those calibrated from the HWM data. This is because the difference in the location of these datasets – quite a few HWMs are around bridges where water channels are narrower than the natural ones.

There is still room to further improve the used regression model to predict roughness values, although improvement upon the traditional method that only uses stream orders to estimate roughness is achieved. The emerging machine learning based models may deliver a better performance, especially involving additional land cover or geographic data.

The Sobel method for locating and merging catchments addressed the discontinuity boundary issues in some areas. However, where one catchment with high Sobel values borders several catchments to be merged, several options exist for determining the order in which catchments should be merged. For our study, we maintained a constant depth before and after merging, but a

more sophisticated approach could be designed to recalculate the rating curves and use a new depth.

We would like to further note that a major challenge to create flood models is still the scarcity of data. The emerging deep learning based model may improve the situation due to its wide coverage and high resolution such as in Wang et al. (2020) and Golparvar and Wang (2020), but the poor data quality should be appropriately addressed.

5 Conclusions

In our research, we aimed to develop flood maps for New Jersey employing the HAND model. By integrating HWM and USGS gauge data, we successfully calibrated the SRCs, though we noted significant variability in the calibrated roughness values. To estimate roughness, we designed a regression model utilizing various catchment data. This regression proved to be more precise than merely relying on stream order for roughness estimation; however, refinement remains possible. Variability in roughness values might be attributed to inaccuracies in NWM flow estimates or SRCs. A notable limitation is that the DEMs, upon which both the HAND data and SRCs are founded, do not account for bathymetry. Addressing this omission or devising compensation strategies emerges as a key area for future research. We also analyzed the influence of different climate scenarios on flooding. It was observed that regions with expansive rivers are more sensitive to changes in precipitation. Specifically, for every 10% increase in precipitation, flood extent typically increased by approximately 2%, although this trend plateaued at higher precipitation levels. To tackle the cross-boundary discontinuity challenge inherent in the HAND, we introduced a method centered on the Sobel filter. Preliminary results indicate that this filter is effective in addressing overall discontinuity.

Competing interests: The authors declare no real or perceived financial conflicts of interest for any author.

Acknowledgments: Funding for the development of the study was provided by the New Jersey Department of Transportation (NJDOT) and the Federal Highway Administration (FHWA) as part of the Region 2 University Transportation Center, hosted by the Center for Advanced Infrastructure and Transportation at Rutgers University. We would like to thank Thomas Suro of USGS, Joseph Ruggeri of NJDEP for providing data and documents related to Hurricane Irene, and the Rutgers Office of Advanced Research Computing (OARC) for providing access to the AMAREL computer cluster.

Open Research: Data archiving is underway for the code and data associated with this project. Figures and data will be available on figshare.com, and code will be available on github.com.
https://figshare.com/authors/David_Bazzett/10942068
https://github.com/dbazzett

References

Anderson, B. J., Brunner, M. I., Slater, L. J., and Dadson, S. J.: (2023) Elasticity curves describe streamflow sensitivity to precipitation across the entire flow distribution, Hydrol. Earth Syst. Sci. Discuss. [Preprint], https://doi.org/10.5194/hess-2022-407, in review.

Afshari, S., Tavakoly, A. A., Rajib, M. A., Follum, M. L., Omranian, E., & Fekete, B. M. (2018). Comparison of new generation low-complexity flood inundation mapping tools with a hydrodynamic model. *Journal of Hydrology*, 556, 539–556. https://doi.org/10.1016/j.jhydrol.2017.11.036

Arnell, N.W., Gosling, S.N. (2016) The impacts of climate change on river flood risk at the global scale. *Climatic Change* **134,** 387–401 . https://doi.org/10.1007/s10584-014-1084-5

Daraio, J. A. (2017). Potential Climate Change Impacts on Streamflow and Recharge in Two Watersheds on the New Jersey Coastal Plain. *Journal of Hydrologic Engineering*, 22(6), 05017002. https://doi.org/10.1061/(ASCE)HE.1943-5584.0001500

DeGaetano, A., & Tran, H. (2021). *Changes in Hourly and Daily Extreme Rainfall Amounts in NJ since the Publication of NOAA Atlas 14 Volume.*

DeGaetano, A., (2021). *Projected Changes in Extreme Rainfall in New Jersey based on an Ensemble of Downscaled Climate Model Projections.*

Gochis, D. J., Dugger, A., McCreight, J., Karsten, L. R., Logan, Yu, W., Pan, L., Yates, D., Zhang, Y., Sampson, K., Cosgrove, B., Salas, F., Clark, E., Graziano, T., Maidment, D., Phan, C., Cui, Z., Liu, Y., Feng, X., and Lee, H.: Technical Description of the National Water Model Implementation of WRF-Hydro, CUAHSI Technical Report, Consortium of Universities for the Advancement of Hydrologic Science, Inc. (CUAHSI), 2016.

Golparvar, B., & Wang, R. Q. (2020, November). AI-supported citizen science to monitor high-tide flooding in Newport beach, California. *Proceedings of the 3rd ACM SIGSPATIAL International Workshop on Advances in Resilient and Intelligent Cities* (pp. 66-69).

Hocini, N., Payrastre, O., Bourgin, F., Gaume, E., Davy, P., Lague, D., Poinsignon, L., & Pons, F. (2020). *Performance of automated flood inundation mapping methods in acontext of flash floods: A comparison of three methods based eitheron the Height Above Nearest Drainage (HAND) concept, or on1D/2D shallow water equations* [Preprint]. Catchment hydrology/Modelling approaches. https://doi.org/10.5194/hess-2020-597

Johnson, J. M., Munasinghe, D., Eyelade, D., & Cohen, S. (2019). An integrated evaluation of the National Water Model (NWM)–Height Above Nearest Drainage (HAND) flood mapping methodology. *Natural Hazards and Earth System Sciences*, *19*(11), 2405–2420. https://doi.org/10.5194/nhess-19-2405-2019

Li, Z (2016) A Framework of ArcGIS-Based Flood Inundation Modeling and Mapping System, ESRI Proceedings, available at: http://proceedings.esri.com/library/userconf/proc16/papers/265_671.pdf (last access: September 2022).

Liu, Yan Y., Tarboton, David G., and Maidment, David R. (2020), Height Above Nearest Drainage (HAND) and Hydraulic Property Table for CONUS - Version 0.2.1. *Oak Ridge Leadership Computing Facility*. DOI: 10.13139/ORNLNCCS/1630903

Liu, Yan Y., Tarboton, David G., and Maidment, David R. (2020), Height Above Nearest Drainage (HAND) and Hydraulic Property Table for CONUS - Version 0.2.0. *Oak Ridge Leadership Computing Facility*. DOI: 10.13139/ORNLNCCS/1608331

Liu, Yan Y., David R. Maidment, David G. Tarboton, Xing Zheng, and Shaowen Wang. (2018) A CyberGIS integration and computation framework for high-resolution continental-scale flood inundation mapping. *JAWRA Journal of the American Water Resources Association* **54**, no. 4: 770-784. DOI: 10.1111/1752-1688.12660

Liu, Y. Y., D. R. Maidment, D. G. Tarboton, X. Zheng, Ahmet Yildirim, N. S. Sazib and S., Wang, (2016), A CyberGIS Approach to Generating High-resolution Height Above Nearest Drainage (HAND) Raster for National Flood Mapping, CyberGIS 16, *The Third International Conference on CyberGIS and Geospatial Data Science*, Urbana, Illinois, July 26-28. http://dx.doi.org/10.13140/RG.2.2.24234.41925

Maidment, D. R. (2017a). Conceptual Framework for the National Flood Interoperability Experiment. *JAWRA Journal of the American Water Resources Association*, *53*(2), 245–257. https://doi.org/10.1111/1752-1688.12474

National Oceanographic and Atmospheric Administration (NOAA) Office of Water Prediction (OWP), (2022), "Inundation Mapping" (also referred to as Flood Inundation Mapping, or FIM), https://github.com/NOAA-OWP/inundation-mapping

Nobre, A. D., Cuartas, L. A., Hodnett, M., Rennó, C. D., Rodrigues, G., Silveira, A., Waterloo, M., & Saleska, S. (2011). Height Above the Nearest Drainage – a hydrologically relevant new terrain model. *Journal of Hydrology*,

404(1), 13–29. https://doi.org/10.1016/j.jhydrol.2011.03.051

Smith, A (2018), *2017 U.S. billion-dollar weather and climate disasters: A historic year in context | NOAA Climate.gov*. Retrieved May 19, 2023, from http://www.climate.gov/disasters-2017

Sobel, I. (2014). An Isotropic 3x3 Image Gradient Operator. *Presentation at Stanford A.I. Project 1968*.

USDA-SCS (1986), Urban Hydrology for Small Watersheds. Technical Release No. 55 (TR-55). USDASCS, Washington DC.

U.S. Geological Survey, (2018), National Hydrography Dataset Plus Attributes (ver. USGS National Hydrography Dataset (NHD) for Hydrologic Unit (HU) 2 - 02 (published 20181119)) accessed January, 2021 at URL https://www.epa.gov/waterdata/nhdplus-mid-atlantic-data-vector-processing-unit-02

Wang, R. Q., Hu, Y., Zhou, Z., & Yang, K. (2020). Tracking flooding phase transitions and establishing a passive hotline with AI-enabled social media data. IEEE Access, 8, 103395-103404.

Watson K., Collenburg J., Reiser R., (2014), Summary of Flooding in New Jersey Caused by Hurricane Irene, August 27–30, 2011, Retrieved May 19, 2023, from https://www.usgs.gov/center-news/summary-flooding-new-jersey-caused-hurricane-irene-august-27-30-2011?qt-news_science_products=7#qt-news_science_products

Xu, D., Bisht, G., Zhou, T., Leung, L. R., & Pan, M. (2022). Development of Land-River Two-Way Hydrologic Coupling for Floodplain Inundation in the Energy Exascale Earth System Model. *Journal of Advances in Modeling Earth Systems*, *14*(8), e2021MS002772. https://doi.org/10.1029/2021MS002772

Zheng, X., Maidment, D. R., Tarboton, D. G., Liu, Y. Y., & Passalacqua, P. (2018). GeoFlood: Large-Scale Flood Inundation Mapping Based on High-Resolution Terrain Analysis. *Water Resources Research*, *54*(12). https://doi.org/10.1029/2018WR023457

Zheng, X., Tarboton, D. G., Maidment, D. R., Liu, Y. Y., & Passalacqua, P. (2018). River Channel Geometry and Rating Curve Estimation Using Height above the Nearest Drainage. *JAWRA Journal of the American Water Resources Association*, *54*(4), 785–806. https://doi.org/10.1111/1752-1688.12661